JOURNAL OF COMPUTATIONAL PHYSICS 107, 1–9 (1993)

Hairpin Removal in Vortex Interactions II*

ALEXANDRE JOEL CHORIN

Department of Mathematics, University of California and Lawrence Berkeley Laboratory, Berkeley, California 94720

Received August 16, 1991; revised August 27, 1992

A vortex method in three dimensions is simplified through the removal of small folds ("hairpins"). The procedure is justified as a real-space renormalization, within a framework provided by recent results on the statistical equilibria of vortex filaments. An application to a vortex ring is carried out. Applications to other numerical methods as well as open questions are discussed.

INTRODUCTION

Three-dimensional inviscid or high-Reynolds number flow is difficult to compute. Ever smaller scales of motion are excited, and all scales are coupled. In most cases, it is impractical to resolve all scales; without a reasonable treatment of the small scales, the accuracy of the calculation soon deteriorates. One would like some way of removing small scales without harming the large scales. In other contexts, such removal can be effected through renormalization.

Recent statistical mechanical analyses of vortex motion [11, 13] provide a justification for the removal of small scales through the removal of "hairpins," i.e., small scale folds in vortex lines. Indeed, they show that an appropriate version of the hairpin removal introduced in [9] constitutes the appropriate modification of the Kosterlitz and Thouless [22, 24] and Shenoy and Williams [34, 37] real-space renormalization to a classical (i.e., non-quantum) fluid in turbulent motion. We shall explain the theory briefly and provide a suitable algorithm. The numerical results support the theory.

From a purely algorithmic point of view, the method described below improves on the hairpin removal of [9] through the use of vortex filaments rather than unconnected vortex segments and through the use of constant cores. The use of filaments requires the introduction of cut-and-paste algorithms that are of interest in other applications.

* This work was supported in part by the Applied Mathematical Sciences subprogram of the Office of Energy Research, U.S. Department of Energy, under Contract DE-AC03-76SF-00098, and in part by the National Science Foundation under Grant Number DMS89-19074.

The theory is directly applicable to calculations based on Buttke's magnetization representation [6]. The algorithms bear a substantial formal resemblance to Dritschel's surgery for contour dynamics in the plane [16, 17]. The main practical differences are related to the fact that vorticity contours in the plane are much smoother than vortex lines in space (see below). However, the theoretical justification raises interesting problems about the statistics of vortex patches. The algorithms also bear some resemblance to the limiters of computational gas dynamics.

Finally, the theory makes contact with the justifications used in other approaches to large-eddy simulation through the observation that the spectrum of the scales that are removed has a Kolmogorov form. The implication of these ideas in a broader context will be discussed.

Our test problem will be the motion of a circular vortex ring, with appropriate perturbations.

THE EQUILIBRIUM THEORY OF VORTEX FILAMENTS

Consider a sparse collection of vortex filaments, as is appropriate for intermittent flow, and assume their lengths are fixed so that thermal equilibrium can be reached [8, 10]. It is enough to consider a single filament. Endow this filament with the appropriate hydrodynamical energy $E=(8\pi)^{-1}\int d\mathbf{x}\int d\mathbf{x}'\,\xi(\mathbf{x})\cdot\xi(\mathbf{x}')/|\mathbf{x}-\mathbf{x}'|$, where $\xi(\mathbf{x})$ is the vorticity at $\mathbf{x}$, and assign to each configuration C of the filament a probability $P(C)\propto\exp(-E/T)$, where T is a temperature that can be positive or negative. A negative temperature is "hotter" than a positive temperature, and $|T|=\infty$ is the boundary between positive and negative temperatures [25].

When $T<0$ the vortex lines are smooth. When $T>0$ vortex filaments collapse into tightly folded structures, and if reconnection is allowed, they break down into small loops. At the boundary $|T|=\infty$ the vortex lines are fractal objects whose axis has fractal dimension $\sim\frac{5}{3}$; the corresponding spectrum has the Kolmogorov form. The average energy of a vortex system is an increasing function of T (remembering that $T<0$ is larger than $T>0$) and of the length L of the filament. In the neighborhood of the $|T|=\infty$ transition a

0021-9991/93 $5.00

vortex system resembles a vortex system near the superfluid/normal fluid quantum transition, where a renormalization procedure is known [12, 13, 22].

Now suppose vortex stretching is allowed. Start with smooth vortex lines ($T<0$). Conservation of energy and the increase in L will force the temperature down, towards $|T|=\infty$. The $|T|=\infty$ threshold is uncrossable for a continuum Euler system, and that is where such a system will remain. A viscous fluid or an underresolved numerical calculation can cross that threshold. This crossing is accompanied by a loss of energy, by reconnection, and by a growth in the fractal dimension of the filaments, and thus by excess vortex stretching and folding. One consequence is that energy loss and reconnection appear simultaneously. Another consequence is that an inaccurate calculation (by a vortex method or indeed by any other), by allowing the crossing of the threshold, will produce too much vorticity and overpredict singularity formation accompanied by energy loss. We no longer believe, in particular, in the reality of the singularity observed in [9].

It goes without saying that in time-dependent problems, where the initial data are smooth and the large-scale features of the flow are time-dependent, the equilibrium and quasi-equilibrium considerations apply only to the small scales of motion.

RENORMALIZATION

The $|T|=\infty$ turbulent state is a critical state, in the sense of the theory of critical phenomena, and it shares many properties with a quantum vortex system at the temperature T_c of the superfluid transition. Indeed, in a model "$2\frac{1}{2}$-dimensional" system one can draw a curve, in an appropriate parameter space, that links these transitions and along which the properties of the system are invariant [12]. It is reasonable to expect that the renormalization analysis near the superfluid transition can shed light on the turbulent state and suggest ways of "renormalizing," i.e., simplifying vortex calculations.

In a renormalization, one repeatedly removes small scales from a calculation in such a way that equilibria or dynamics are unchanged on much larger scales. Assume that the small scales are in approximate thermal equilibrium, and suppose to begin with that the temperature T is finite and positive. When $T>0$, a large vortex loop "polarizes" smaller ones, i.e., the greater likelihood of lower energies in a canonical distribution with $T>0$ makes it likely that smaller loops are arranged so as to reduce the energy. The removal of small scale structures requires a decrease in vortex strength to make up for it. For $T<0$, the opposite is true: at or near equilibrium a large loop "anti-polarizes" smaller ones, and renormalization requires the strengthening of remaining vortex lines. On the $|T|=\infty$ boundary between positive and negative temperatures one should be able to remove small scales with impurity and leave the vortex strengths invariant. The removal of small scales is the goal of hairpin removal.

Another parameter that has to be "renormalized" is the "chemical potential" that is a function of vortex core size [12]. A similar argument can be made to show that the vortex core size should remain fixed as well, as has been discovered by extensive numerical experimentation [31]. This conclusion is somewhat counterintuitive, and the opposite was assumed in [9], to the detriment of accuracy.

Renormalization keeps invariant an ensemble, and we wish to keep invariant the large-scale behavior of a single flow. The gap between the two can be bridged by noting that a single flow can be viewed as a union of subflows, each in approximate thermal equilibrium with the rest. Thus we expect that the small scale loops or folds that are generated in an inviscid calculation have orientations that are statistically independent of the large scales. The removal of small scales is not necessarily without penalty, since it is equivalent to a sum of small changes whose average is zero but which are not zero individually. The resulting collection of perturbations should have a slightly viscous effect that is presumably small in comparison with the viscous effect of underresolved differencing on a grid.

Note that hairpin removal can be justified only if the calculation is accurate enough to remain near $|T|=\infty$ and not to fold further into the positive T regime.

There is a natural connection between hairpin removal and other approaches to large eddy simulation, inasmuch as the removal leaves invariant the large $|T|$ regime and thus keeps invariant the Kolmogorov spectrum at high wave numbers k, even beyond the level of resolution.

RELATION WITH CONTOUR SURGERY IN THE PLANE

The removal of hairpins, which we shall see involves reconnections of vortex lines, bears at least a philosophical resemblance to surgery performed on vortex contours in two-dimensional flow, as presented in [16]. The practical details are perforce different, as a consequence of the difference in smoothness between two-dimensional contours and three-dimensional nearly fractal vortex lines. In [17], contour surgery is justified on the basis of a cascade argument that resembles the standard cascade analysis of the three-dimensional flow.

It would appear that surgery requires the statistical independence of large scales and small scales, and that in turn requires the infinite temperature that results from an ever increasing number of active scales. However, our present understanding of the statistical mechanics of two-dimensional flow [18, 28, 32] indicates that in two dimensions vortex equilibria are large-scale, the small scales

are asymptotically insignificant, and the temperature remains constant. One could justify two-dimensional surgery by one or both of the following arguments:

(i) One could introduce a scale-dependent temperature and possibly conclude that vorticity contours are controlled by small scales for which a cascade argument holds, leading to infinite temperatures on the scales of the surgery, or/and

(ii) one could argue that the dynamics of the small scales are asymptotically insignificant and thus surgery in two dimensions is harmless because the mishandling of small scales is unimportant.

Thus, the statistical analysis of the constructions in Ref. [16] remains to be carried out.

A VORTEX METHOD FOR EULER'S EQUATIONS

The Euler equations for a fluid of constant density 1 can be written in the form

$$\frac{d\mathbf{x}}{dt}=\mathbf{u}, \qquad \frac{d\xi}{dt}=(\xi\cdot\nabla)\mathbf{u}, \qquad \text{(1a), (1b)}$$

$$\mathbf{u}=K*\xi, \qquad \text{(1c)}$$

where $\mathbf{x}$ is a lagrangian marker moving with the fluid, $\mathbf{u}=\mathbf{u}(\mathbf{x}, t)$ is the velocity, $\xi=\operatorname{curl}\mathbf{u}$ is the vorticity, and K is the operator $K=-(4\pi|\mathbf{x}|^3)^{-1}\mathbf{x}\times$, where $\times$ denotes a cross product and $*$ denotes convolution; i.e., (1c) is a shorthand for

$$\mathbf{u}(\mathbf{x}, t)=-\frac{1}{4\pi}\int d\mathbf{x}'\,\frac{1}{|\mathbf{x}-\mathbf{x}'|^3}(\mathbf{x}-\mathbf{x}')\times\xi(\mathbf{x}'),$$

For a derivation, see, e.g., [14]. Vortex methods are Lagrangian discretizations of these equations. The variant proposed here is nearly identical to the one in [7]; the main difference is the use of higher-order cores and higher-order time integration. For other examples of vortex methods and for theory, see, e.g., [1, 3–5, 19, 23, 26].

Approximate the vorticity field ξ by a finite collection of closed vortex loops S_i, each with circulation κ_i, $i=1, \ldots, N$. Place n_i points $\mathbf{x}_1, \mathbf{x}_2, \ldots, \mathbf{x}_{n_i}$, on the ith loop. Approximate the loop S_i by the n_i segments $\overline{\mathbf{x}_{n_i}\mathbf{x}_1}$, $\overline{\mathbf{x}_1\mathbf{x}_2}$, $\overline{\mathbf{x}_{n_i-1}\mathbf{x}_{n_i}}$. Let $\mathbf{s}_j$ be the jth of these segments, $\mathbf{s}_j=\mathbf{x}_j-\mathbf{x}_{j'}$, $j'=j-1$ if $j\neq 1$, $j'=n_i$ if $j=1$. The use of closed loops guarantees that in an appropriate sense $\operatorname{div}\xi=0$ (the slight ambiguity in this statement is analyzed in, e.g., [30]; the importance of satisfying $\operatorname{div}\xi=0$ is analyzed in [6]). Ensure that the lengths of the $\mathbf{s}_j$ satisfy $|\mathbf{s}_j|\leqslant h$, h a predetermined bound. Note that a reversal in the sign of κ_i and an appropriate renumbering of the $\mathbf{x}_j$ leaves the vorticity in S_i invariant; to avoid this ambiguity, make all the κ_i positive. For ease of reconnection (see below) it is convenient to pick all κ_i equal, $\kappa_i=\kappa$ for all i.

Let $\mathbf{x}_j^m=\frac{1}{2}(\mathbf{x}_j+\mathbf{x}_{j'})$ be the center of the jth segment. The velocity at a point $\mathbf{x}$ is the following discrete version of (1c):

$$\mathbf{u}(\mathbf{x}, t)=-\frac{\kappa}{4\pi}\sum_j\frac{\mathbf{r}_j\times\mathbf{s}_j}{|\mathbf{r}_j|^3}f(|\mathbf{r}_j|/\sigma), \qquad (2)$$

where the sum is over all segments on all loops, $\mathbf{r}_j=\mathbf{x}_j^m-\mathbf{x}$, f is a core function chosen so as to enhance accuracy [5, 21], and σ is the cutoff length that can serve as a measure of the thickness of the loops and is constant in time. σ should be larger than the typical distance between neighboring segments. We shall use the fourth-order core function $f(q)=(1-(1-\frac{3}{2}q^3))\,e^{-q^3}$. The calculated $\mathbf{u}(\mathbf{x}_j)$ is used to advance $\mathbf{x}_j$. The variation in the lengths of the segments as a result of the motion of their end-points automatically satisfies Eq. (1b). The ordinary differential equations (1a) will be solved by a fourth-order Runge–Kutta method with time step k adjusted so that $k\cdot\max|\mathbf{u}(\mathbf{x}_j)|\leqslant\Delta$, Δ a controllable parameter (see more below). If the length of a segment exceeds h, the segment is cut into two, with the coordinates of the new point found by linear interpolation.

It may seem surprising that while we use fourth-order integration in time and a fourth-order core, the integration along filaments (2) and the interpolation just mentioned are first-order accurate only. Numerical experiment shows that higher-order integration and higher-order interpolation along filaments detract from accuracy, except when a single filament is used or when the vorticity has not yet stretched. The reason should probably be sought in the lack of smoothness of vortex filaments, as discussed above. In addition, the difference between the result of linear interpolation for segment splitting and the result of higher-order interpolation is a small loop and presumably unimportant when the vortex is sufficiently stretched. On the other hand, the usefulness of higher-order time integration and of higher-order cutoffs is consistent with the smoothness of the lagrangian flow map [20].

Integrals of motion can be used to provide partial information about the accuracy of the calculation. The three components I_1, I_2, I_3 of the impulse $\mathbf{I}=\int\mathbf{x}\times\xi\,d\mathbf{x}$ can be approximated by

$$\mathbf{I}\cong\sum_i\mathbf{x}_i^m\times\kappa\mathbf{s}_i,$$

and the energy E can be approximated as

$$E=\frac{\kappa^2}{8\pi}\sum_i\sum_{j\neq i}\frac{\mathbf{s}_i\cdot\mathbf{s}_j}{|\mathbf{x}_i^m-\mathbf{x}_j^m|}+\frac{\kappa^2}{8\pi}\sum_i E_{ii},$$

where the first term is the interaction energy and the second

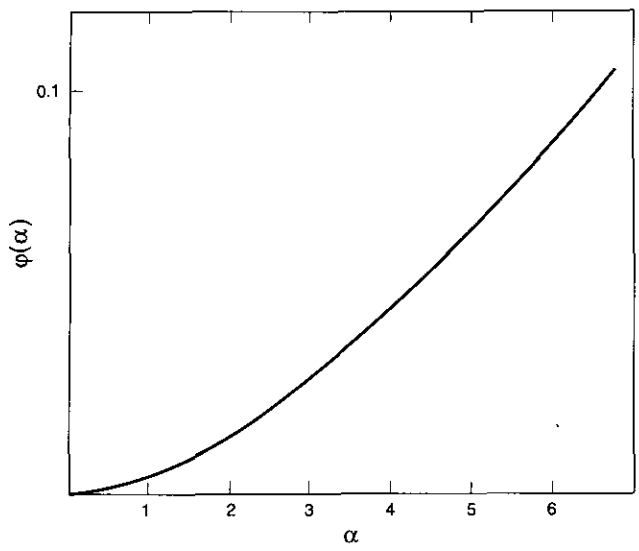

FIG. 1. Self-energy function ϕ.

term is the "self-energy," which is small when the number of segments n is large or when the vortex lines are smooth. The self-energy can be evaluated through the relations [8]

$$E_{ii}(|\mathbf{s}_i|, \sigma) = \sigma E_{ii}\left(\frac{|\mathbf{s}_i|}{\sigma}\right) = \sigma\phi\left(\frac{|\mathbf{s}_i|}{\sigma}\right),$$

where ϕ is a function of a single variable that depends on the cutoff function f and which can be evaluated once and for all for any given f and stored (see [8, 31]). The ϕ we use is sketched in Fig. 1. Its asymptotic properties for small or large arguments are independent of f (see [8]) and a change in f does not change ϕ much. The main remaining source of error in the approximation of E above is the fact that the interaction energy as written is a rough approximation for nearby segments.

HAIRPIN REMOVAL AND RECONNECTION

We now wish to remove small hairpins in a vortex calculation; a large vortex with a small hairpin can be viewed as a smooth vortex with an adjacent small vortex loop, so that our renormalization argument applies.

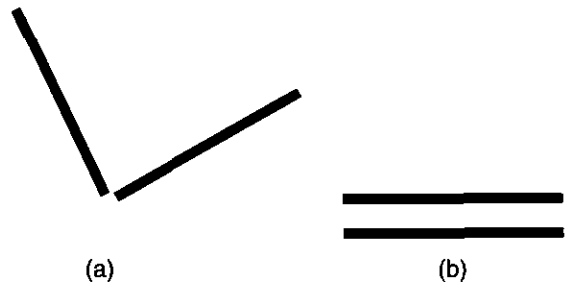

FIG. 2. Relative configuration of two vortex segments.

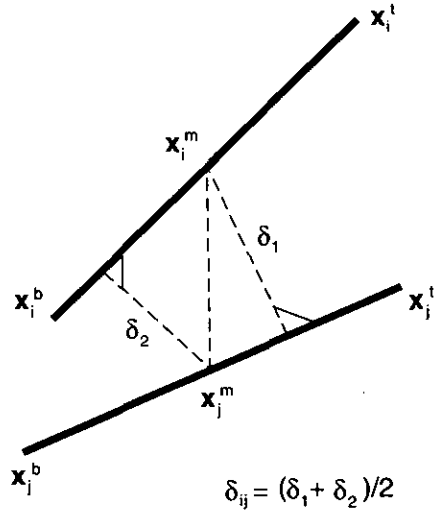

FIG. 3. Distance between segments.

Consider two adjacent segments on the same numerical vortex loop. Suppose the angle between them is large. The addition of the two segments will then remove a small hairpin. Note that this is different from maintaining the smoothness of the vortex filament at all times (for example, through a repeated use of spline smoothing) inasmuch as stretching and folding are allowed and the smoothing appears only after a substantial amount of folding has occurred and the temperature thus presumably has decreased to the neighborhood of infinity.

The angle between the adjacent segments is $\cos\theta = (\mathbf{s}_i \cdot \mathbf{s}_{i'})/(|\mathbf{s}_i| \cdot |\mathbf{s}_{i'}|)$, where i, i' are the appropriate indices. The angle will be viewed as too large when $\cos\theta < (\cos\theta)_{\min}$, where $(\cos\theta)_{\min}$ is a predetermined parameter. When the angle is too large, the pair is replaced by the sum and the filament remains connected. This process reduces the length of vortex lines and is the improved version of the hairpin removal of Ref. [9].

The parameter $(\cos\theta)_{\min}$ determines the size of the hairpins that are removed. The large scale numerical results should be independent of $(\cos\theta)_{\min}$ once the latter is small enough, but the number of segments in the calculation should decrease as $(\cos\theta)_{\min}$ is decreased.

One may also wish to remove hairpins that appear when

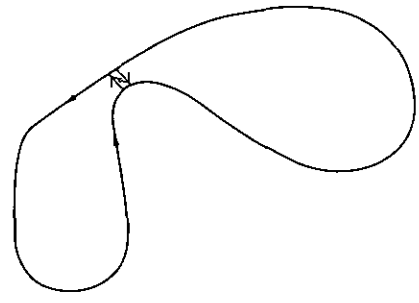

FIG. 4. Splitting a filament into two.

nearby counterrotating segments approach each other without being adjacent on a filament or even without being on the same filament. To remove them, one should reconnect the filaments. Such a reconnection is mainly a bookkeeping operation and is not necessarily accompanied by a physical vortex reconnection [2]. Presumably, a numerical description of a physical reconnection would involve many "bookkeeping" reconnections.

Reconnection occurs when two segments, say with indices i and j, are such that the angle θ between them satisfies $\cos\theta < (\cos\theta)_{\min}$, and they are close to each other. To find such segments, one has to define the distance between segments. This is not trivial, because a reasonable definition of distance must take into account not only the minimum or the maximum distance between them, but also their relative configuration. Thus, in Fig. 2, the two elements in case (a) are further from each other than the elements in case (b), even though their minimum distance is smaller.

Consider the segments i, j in Fig. 3. We shall be interested in their distance δ_{ij} only if it is small. If $|\mathbf{x}_i^m - \mathbf{x}_j^m|$, the distance between their centers, is larger than h, the bound on segment length, we set $\delta_{ij} = |\mathbf{x}_i^m - \mathbf{x}_j^m|$. Otherwise, we define δ_1 to be the length of the projection of the line of centers on that normal to segment i that lies in the plane through the centerline of segment j and the point $\mathbf{x}_i^m$ and similarly define δ_2 to be the length of the projection of the line of centers on that normal to segment i that lies in the plane through segment j and $\mathbf{x}_j^m$. We then set $\delta_{ij} = \frac{1}{2}(\delta_1 + \delta_2)$. This definition of δ_{ij} is the symmetrized version of the one in Ref. [9].

We now define two operations on filaments: splitting a filament into two, and merging two filaments into one. Consider a filament as in Fig. 4. If two non-adjoining segments of the filament satisfy the conditions: (i) $\delta_{ij} \prec \delta_{\min}$, (ii) $\cos\theta_{ij} \equiv (\mathbf{s}_i \cdot \mathbf{s}_j)/(|\mathbf{s}_i|\,|\mathbf{s}_j|) < (\cos\theta)_{\min}$ (where $(\cos\theta)_{\min}$ and $\delta_{\min}$ are predetermined bounds), the filament will be split into two through the addition of two neighboring counterrotating segment as shown in the figure. This splitting does not change the vorticity or velocity fields in the absence of further manipulations. Similarly, if two segments belonging to two different filaments satisfy the two same conditions, their filaments will be reconnected into one as in Fig. 5. Note that we are not interested in reconnection if $\mathbf{s}_i$, $\mathbf{s}_j$ point approximately in the same direction. In a time-dependent calculation, any one filament will not be allowed to participate in a reconnection more than once per time step; since the criteria for splitting or reconnecting are the same, this condition must be enforced by some logical programming. In general, we pick $\delta_{\min} = \frac{1}{5}h$.

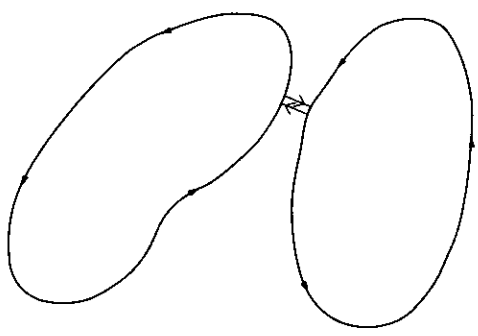

FIG. 5. Reconnecting two filaments into one.

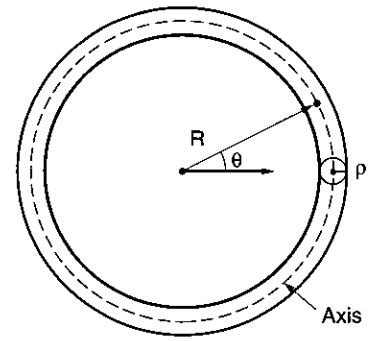

FIG. 6. A vortex ring.

A NUMERICAL EXAMPLE: THE MOTION OF A PERTURBED VORTEX RING

To illustrate the constructions above and show their usefulness we consider the evolution of a vortex ring with ring radius R and arm radius ρ (Fig. 6). Initially the ring is kicked by a localized, smooth, finite amplitude perturbation (Fig. 8a). A study of a ring with small periodic perturbations has been carried out in [23]; if the initial perturbations are small it takes a long time for hairpin removal to become significant and our methodology has little to add to the stability analysis in [23].

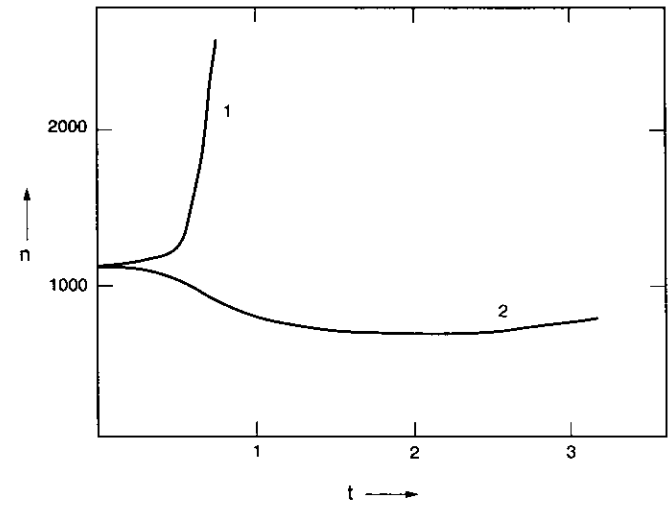

FIG. 7. Growth of the number of segments in time: Curve 1 without hairpin removal; curve 2 with hairpin removal.

There is a clear connection between the accuracy of the underlying algorithm and the number of hairpins that are removed. According to the theory above, when a calculation is inaccurate it can slip below the $|T| = \infty$ threshold, overestimate the amount of stretching and folding, and create additional hairpins. This relationship is observed in practice.

We approximate the perturbed ring by N filaments placed in the arms of the ring in such a way that each is surrounded by an equal volume. Each filament starts with n_0 segments, so that at $t = 0$ there are $n = Nn_0$ segments. In addition to removing hairpins, we remove very small segments ($|\mathbf{s}_i| \leqslant \frac{1}{10}h$).

In Table I we display the results of a calculation with $N = 19$, $n_0 = 60$, $\rho/R = 0.277$. Δ, the time stepping parameter that bounds k max $|\mathbf{u}|$, k = time step, is taken equal to the

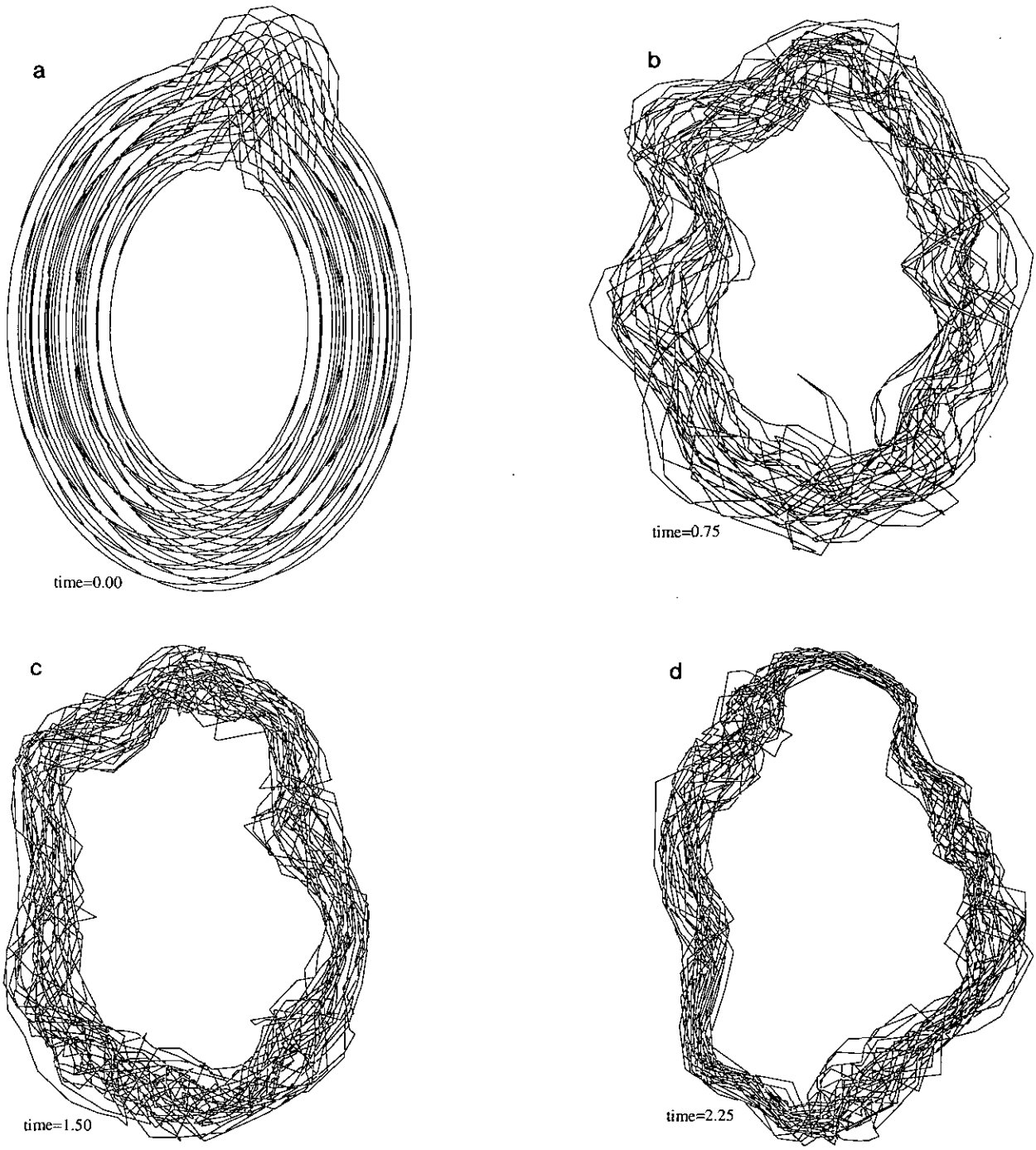

FIG. 8. The evolution of a vortex ring: (a) $t = 0$; (b) $t = 0.75$; (c) $t = 1.50$, (d) $t = 2.25$.

smallest distance between segment centers. Δ is, in fact, the most sensitive numerical parameter, since it must be small enough to ensure that the rotation in the arms is accurately represented [29]. To ease this problem we picked the relatively large ratio of ρ to R. The test for hairpin removal uses $(\cos\theta)_{\min} = 0$, i.e., hairpin removal occurs if neighboring segments attempt to form a right angle. The cutoff length σ is 2.5 times the largest initial distance between neighboring segments. The bound on segment length, h, is $\frac{3}{2}$ of the largest initial segment length. We display the number of steps, the number n of segments in the calculation at that step, the cumulative total n_1 of segments removed, the time elapsed, the computed energy, the impulse in the direction of motion, and the impulse in an orthogonal direction. In Table II we display the result of an attempt to carry out the same calculation without hairpin removal ($n_1 \equiv 0$). The integrals of motion are conserved, if anything, better with than without hairpin removal. Without hairpin removal the number of segments in the calculation increases very fast and the calculation must be stopped. With hairpin removal n begins by declining, as a result of the fact that the initial segment lengths are smaller than the maximum allowed, and with the removal of small segments there is room for expansion. The difference in the values of n as functions of

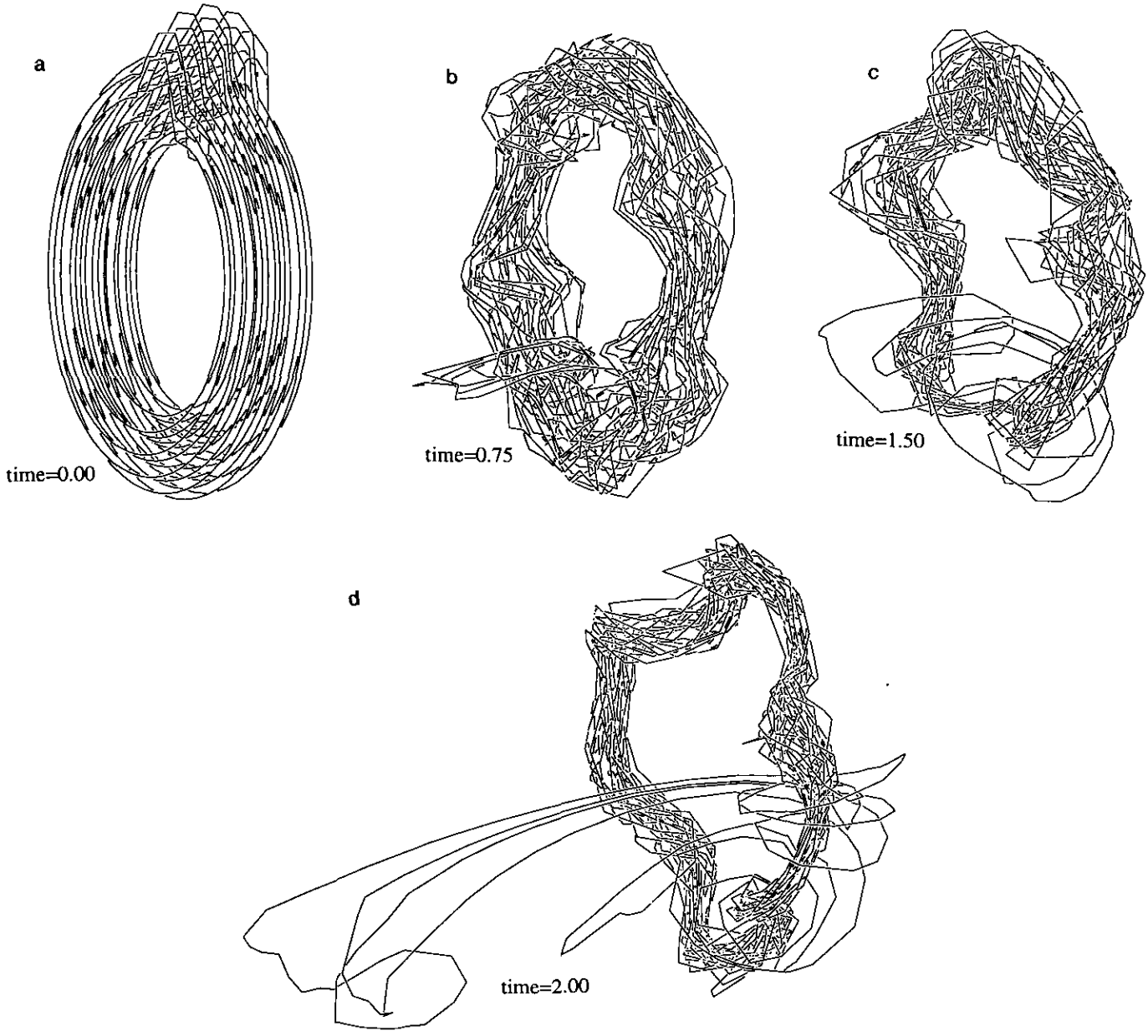

FIG. 9. Evolution of a vortex ring, large time step: (a) $t = 0$, (b) $t = 0.75$, (c) $t = 1.50$, (d) $t = 2.00$.

TABLE I

Calculation with Hairpin Removal

Step	n	n_1	Time	Energy	Impulse-x	Impulse-y
0	1140	0	0.0	0.102	0.213	0.0
100	1110	52	0.340	0.101	0.212	−0.001
200	942	305	0.670	0.100	0.211	−0.001
300	792	789	0.986	0.104	0.212	−0.004
400	738	1113	1.284	0.103	0.207	−0.006
500	730	1457	1.588	0.103	0.206	−0.005
600	692	1822	1.903	0.104	0.204	0.001
700	669	2058	2.225	0.107	0.208	0.004
800	669	2208	2.551	0.107	0.209	0.014
900	881	2917	3.003	0.107	0.212	0.001

the time t is displayed in Fig. 7. Curve (1) (no removal) is familiar from other vortex calculations [7, 23].

In both runs we start with $N = 19$, $n_0 = 60$. The calculated velocity of the ring is 5% above the value predicted by the asymptotic formula $U = (\log(8R/\rho) - 0.25)/4\pi R + O(\rho/R)$, see [33]. Since ρ/R is not small here, and the numerical representation of ρ is only approximate because it is not clear how σ contributes to it, this is an adequate agreement. Computer analyses of the convergence of vortex methods in three space dimensions can be found in Refs. [1, 23]; our goal here is only to contrast calculations with and without hairpin removal.

Good conservation properties and a correct evaluation of a global quantity such as ring velocity do not guarantee accuracy. To see what the calculation looks like, we reproduce in Fig. 8 a run with $N = 31$, $n_0 = 70$, $(\cos\theta)_{\min} = 0$, and other parameters chosen as per the considerations above. In Fig. 8a the ring with the initial bump is shown. The other figures are at $t = 0.75$, $t = 1.50$, $t = 2.25$. The initial bump resolves itself into waves moving on the ring. The six cornered configuration, predicted by linear stability theory [23, 35], by earlier calculations [23], and by the study of model problems [15], can be discerned. The ring retains its topological integrity for a long time, as observed in experiments [27, 33]. Eventually, vorticity begins to shoot off into the wake, roughly at the antipode position from the initial perturbation. The hairpin removal deletes most of the thin arms that are thus produced; the impulse is well conserved. This sequence of events is plausible to anyone who has watched a smoke ring and is consistent with the photographs in [36] and also in [33], when only axisymmetric flows are considered.

TABLE II

Calculation without Hairpin Removal

Step	n	Time	Energy	Impulse-x	Impulse-y
0	1140	0.0	0.102	0.213	0.0
50	1161	0.163	0.102	0.213	−0.001
100	1189	0.327	0.101	0.214	−0.003
150	1295	0.485	0.102	0.218	−0.004
200	2401	0.743	0.104	0.229	−0.004

To exhibit the shedding of vorticity that is being deleted, we exhibit in Fig. 9 a calculation with $n_0 = 60$ and a time step four times larger than in Fig. 8. The hairpin removal occurs four times less frequently and is thus less efficient. The shedding explains the thinning of the visible ring. The energy and impulse are very accurately preserved in all these calculations. The increase in energy due to the thinning of the ring is balanced by the folding of the filaments. The main obstacle to longer runs is the need for small time steps. (It took about 1000 time steps to get to $t = 2.25$ in Fig. 8.) A time step that is too large detracts from accuracy; its effect on the number of hairpins present is not large.

Eventually the ring collapses into a complicated tangle; by that time the accuracy of the calculation, as determined by comparing runs with different parameter values, is not high and it is not clear how seriously the details should be taken. The collapse is not reproduced here.

CONCLUSION

Figure 7, together with Tables I, II, is our main result. Without a visible loss of accuracy on the large scales, the growth in the number of segments and in the complexity of small scales has been at least partially tamed.

Our procedure removes small scales from a vortex calculations and is possibly related to the contour surgery of [16]. The key observation that leads to a justification is that flow with stretched vorticity lives near an infinite temperature. We work directly with the computer representation of the solution, and no effort is made to derive auxiliary "effective" differential equations.

An interesting question that remains open is how to apply our theory in the context of other numerical methods, for example, finite difference methods. Underresolution and numerical viscosity also remove small scales in grid-based methods, but they do it differently and certainly not harmlessly. They fatten vortices and thus change the chemical potential, and they average vorticity independently of its orientation. The pictures that result are very different from Fig. 8, where a lot of small-scale structure survives. Clearly, some ways of removing small-scale structure are more legitimate than others on a grid and a clear characterization of what is allowed and what is not would be very helpful.

Note. The program used above is available from the author.

ACKNOWLEDGMENT

I thank T. Ligocki with help in running the calculations.

REFERENCES

1. A. Almgren, T. Buttke, and P. Colella, A fast vortex method in three dimensions, *J. Comput. Phys.* **106**, No. 2 (1993).
2. C. Anderson and C. Greengard, *Comm. Pure Appl. Math.* **42**, 1123 (1989).
3. C. Anderson and C. Greengard, *Vortex methods*, Lecture Notes in Mathematics, Vol. 1360 (Springer-Verlag, New York/Berlin, 1988).
4. J. T. Beale and A. Majda, *Math. Comput.* **32**, 29 (1982).
5. J. T. Beale and A. Majda, *J. Comput. Phys.* **58**, 188 (1985).
6. T. Buttke, Hamiltonian structure of three dimensional incompressible flow, *Comm. Pure Appl. Math.*, in press.
7. A. J. Chorin, *Commun. Math. Phys.* **83**, 517 (1982).
8. A. J. Chorin, *Commun. Math. Phys.* **114**, 167 (1988).
9. A. J. Chorin, *J. Comput. Phys.* **91**, 1 (1990).
10. A. J. Chorin, Lectures in Applied Mathematics, Vol. 28, p. 85 (Am. Math. Soc., Providence, RI, 1991).
11. A. J. Chorin, *Commun. Math. Phys.* **141**, 619 (1991).
12. A. J. Chorin, *J. Statist. Phys.* **69**, 67 (1992).
13. A. J. Chorin and J. Akao, *Physica D.* **52**, 403 (1991).
14. A. J. Chorin and J. Marsden, *A Mathematical Introduction to Fluid Mechanics* (Springer-Verlag, New York/Berlin, 1979, 1990).
15. J. Cieslinski, P. Gragert, and A. Sym, *Phys. Rev. Lett.* **57**, 1507 (1986).
16. D. Dritschel, *J. Comput. Phys.* **77**, 240 (1988).
17. D. Dritschel, *J. Fluid Mech.* **194**, 511 (1988).
18. G. Eyink and H. Spohn, *J. Statist. Phys.*, in press.
19. C. Greengard, *Math. Comput.* **47**, 387 (1986).
20. O. H. Hald, manuscript, 1987.
21. O. H. Hald, *SIAM J. Numer. Anal.* **24**, 538 (1987).
22. C. Itzykson and J. M. Drouffe, *Statistical field theory* (Cambridge Univ. Press, New York, 1989).
23. O. Knio and A. Ghoniem, *J. Comput. Phys.* **86**, 75 (1990).
24. J. Kosterlitz and D. J. Thouless, *J. Phys. C: Solid State Phys.* **6**, 1181 (1973).
25. L. Landau and E. Lifshitz, *Statistical Physics, Part* 1 (Pergamon, New York, 1980).
26. A. Leonard, *Annu. Rev. Fluid Mech.* **17**, 523 (1985).
27. T. Maxworthy, *J. Fluid Mech.* **64**, 227 (1974).
28. J. Miller, *Phys. Rev. Lett.* **65**, 2137 (1990).
29. M. Perlman, *J. Comput. Phys.* **59**, 200 (1985).
30. E. G. Puckett, "A Review of Vortex Methods," in *Incompressible Computational Fluid Mechanics*, edited by R. Nicolaides and M. Gunzberger (Cambridge Univ. Press, New York, 1992).
31. A. Qi, Ph.D. thesis, Math. Dept., UC Berkeley, 1991.
32. R. Robert, *J. Statist. Phys.* **65**, 531 (1991).
33. K. Shariff and A. Leonard, *Annu. Rev. Fluid Mech.* **24**, 235 (1992).
34. S. R. Shenoy, *Phys. Rev. B* **40**, 5056 (1989).
35. S. Widnall, *Annu. Rev. Fluid Mech.* **8**, 141 (1976).
36. M. van Dyke, *An Album of Fluid Motion* (Parabolic Press, Stanford, 1982), p. 66.
37. G. Williams, *Phys. Rev. Lett.* **59**, 1926 (1987).